

This is the accepted manuscript made available via CHORUS. The article has been published as:

Measurement of the -3 keV Resonance in the Reaction $^{13}\text{C}(\alpha, n)^{16}\text{O}$ of Importance in the s-Process

M. La Cognata, C. Spitaleri, O. Trippella, G. G. Kiss, G. V. Rogachev, A. M.

Mukhamedzhanov, M. Avila, G. L. Guardo, E. Koshchiy, A. Kuchera, L. Lamia, S. M. R.

Puglia, S. Romano, D. Santiago, and R. Spartà

Phys. Rev. Lett. **109**, 232701 — Published 4 December 2012

DOI: [10.1103/PhysRevLett.109.232701](https://doi.org/10.1103/PhysRevLett.109.232701)

Measurement of the -3 keV resonance in the reaction $^{13}\text{C}(\alpha, n)^{16}\text{O}$ of importance in the s-process.

M. La Cognata^{1,*}, C. Spitaleri^{1,2}, O. Trippella^{1,3}, G.G. Kiss^{1,4}, G.V. Rogachev⁵,
A.M. Mukhamedzhanov⁶, M. Avila⁵, G.L. Guardo^{1,2}, E. Koshchiy⁵, A. Kuchera⁵,

L. Lamia², S.M.R. Puglia^{1,2}, S. Romano^{1,2}, D. Santiago⁵, and R. Sparta^{1,2}

¹*Istituto Nazionale di Fisica Nucleare, Laboratori Nazionali del Sud, Catania, Italy*

²*Dipartimento di Fisica e Astronomia, Università di Catania, Catania, Italy*

³*Istituto Nazionale di Fisica Nucleare, Sezione di Perugia,*

⁴*Dipartimento di Fisica, Università di Perugia, Perugia, Italy*

⁵*Institute of Nuclear Research (ATOMKI), Debrecen, Hungary*

⁶*Department of Physics, Florida State University, Tallahassee, Florida, USA*

⁶*Cyclotron Institute, Texas A&M University, College Station, Texas, USA*

The $^{13}\text{C}(\alpha, n)^{16}\text{O}$ reaction is the neutron source for the main component of the s-process, responsible of the production of most nuclei in the mass range $90 \lesssim A \lesssim 204$. It is active inside the helium-burning shell in asymptotic giant branch stars, at temperatures $\lesssim 10^8$ K, corresponding to an energy interval where the $^{13}\text{C}(\alpha, n)^{16}\text{O}$ is effective of 140 – 230 keV. In this region, the astrophysical S(E)-factor is dominated by the -3 keV sub-threshold resonance due to the 6.356 MeV level in ^{17}O , giving rise to a steep increase of the S-factor. Notwithstanding it plays a crucial role in astrophysics, no direct measurements exist inside the s-process energy window. The magnitude of its contribution is still controversial as extrapolations, e.g. through the R-matrix, and indirect techniques such as the asymptotic normalization coefficient (ANC) yield inconsistent results. The discrepancy amounts to a factor of 3 or more right at astrophysical energies. Therefore, we have applied the Trojan Horse Method to the $^{13}\text{C}(^6\text{Li}, n^{16}\text{O})d$ quasi-free reaction to achieve an experimental estimate of such contribution. For the first time, the ANC for the 6.356 MeV level has been deduced through the THM as well as the n -partial width, allowing to attain an unprecedented accuracy in the $^{13}\text{C}(\alpha, n)^{16}\text{O}$ study. Though a larger ANC for the 6.356 MeV level is measured, our experimental S(E) factor agrees with the most recent extrapolation in the literature in the 140 – 230 keV energy interval, the accuracy being greatly enhanced thanks to this innovative approach.

PACS numbers: 25.70.Hi, 25.55.-e, 26.20.Kn, 95.85.Ry

The origin of chemical elements has been subject of quantitative investigations since the born of modern physics. Regarding $90 \lesssim A \lesssim 204$ nuclei, a major nucleosynthesis site has been identified in low-mass ($\lesssim 3M_{\odot}$) asymptotic giant branch (AGB) stars [1], responsible for the production of heavy elements along the stability valley through slow neutron captures (s-process) [2]. In these stars, protons mixed downward following the quenching of the H-burning shell are quickly captured by carbon nuclei, eventually leading to the formation of a ^{13}C pocket [3]. Then, ^{13}C nuclei give up their excess neutrons to heavier nuclei through the $^{13}\text{C}(\alpha, n)^{16}\text{O}$ reaction, at temperatures varying between $0.8 \cdot 10^8$ K and $1 \cdot 10^8$ K [4]. At $0.9 \cdot 10^8$ K, the energy range where the $^{13}\text{C}(\alpha, n)^{16}\text{O}$ reaction is most effective, the Gamow window [5], is $\sim 140 - 230$ keV. In such region, its direct measurement is exceedingly challenging because of the Coulomb barrier, exponentially suppressing the cross section, and the interplay between the -3 keV resonance and atomic electron screening [6].

The most recent work on the $^{13}\text{C}(\alpha, n)^{16}\text{O}$ [7] combines a high accuracy measurement of its cross section down to 300 keV with an extensive R-matrix fitting of all cross section data for channels feeding ^{17}O states. The high accuracy cross section is used to renormalize previous

$^{13}\text{C}(\alpha, n)^{16}\text{O}$ data sets as they show a $\sim 100\%$ scatter in their absolute values below 1 MeV [7]. The R-matrix fit is used to extrapolate the $^{13}\text{C}(\alpha, n)^{16}\text{O}$ astrophysical factor down to ~ 100 keV to cover the Gamow window. Indeed, at ~ 300 keV the $^{13}\text{C}(\alpha, n)^{16}\text{O}$ cross section is $\sim 10^{-10}$ b, making its measurement extremely difficult. Moreover, electron screening determines a S(E) increase less than 20% [8]. Since our current understanding of electron screening is rather incomplete, potential systematic errors might arise in the extraction of the bare nucleus cross section [9]. Though the R-matrix in [7] improved the determination of the -3 keV resonance tail, global fitting might be inaccurate right at astrophysical energies because of unconstrained variations of some physical parameters [10]. Finally, discrepancies with other R-matrix calculations [11] (in agreement with NACRE extrapolation [12]) and with advanced theoretical calculations, as the microscopic two-cluster model [13], suggest an incomplete knowledge of the low-energy $^{13}\text{C}(\alpha, n)^{16}\text{O}$ S(E)-factor.

Alternative approaches using indirect methods have been undertaken to determine the 6.356 MeV ^{17}O state parameters, in particular the measurement of the asymptotic normalization coefficient (ANC) [18] and of the spectroscopic factor (which pin down the resonance top

TABLE I. Summary of ANC values $(\tilde{C}_{\alpha^{13}\text{C}}^{17\text{O}(1/2^+)})^2$ and of the spectroscopic factors S_α in the literature

Refs.	$(\tilde{C}_{\alpha^{13}\text{C}}^{17\text{O}(1/2^+)})^2$ (fm ⁻¹)	S_α
[14]	0.89 ± 0.23	-
[15]	-	0.01
[16]	-	0.36-0.40
[17]	4.5 ± 2.2	0.29 ± 0.11
this work	$6.7^{+0.9}_{-0.6}$	-

value), to calculate its contribution to the S(E)-factor. The results are summarized in Tab.I. Johnson et al. [14] inferred the ANC of the -3 keV resonance through the $^6\text{Li}(^{13}\text{C}, d)^{17}\text{O}$ sub-Coulomb α -transfer, obtaining $(\tilde{C}_{\alpha^{13}\text{C}}^{17\text{O}(1/2^+)})^2 = 0.89 \pm 0.23 \text{ fm}^{-1}$. Assuming the Γ_n value in the literature [19], a much smaller contribution than in [7, 12] was found. Kubono et al. [15] suggested a very small $S_\alpha = 0.01$ based on their measured $^{13}\text{C}(^6\text{Li}, d)^{17}\text{O}$ transfer reaction. However, a later analysis of their data indicated a considerably stronger contribution [16], $S_\alpha = 0.36 - 0.40$ depending on the theoretical approach. Pellegriti et al. [17] used their $S_\alpha = 0.29 \pm 0.11$, measured through the $^{13}\text{C}(^7\text{Li}, t)^{17}\text{O}$ transfer reaction, to evaluate the ANC, obtaining $(\tilde{C}_{\alpha^{13}\text{C}}^{17\text{O}(1/2^+)})^2 = 4.5 \pm 2.2 \text{ fm}^{-1}$, five times higher than the one in [14]. Introducing the ANC into a R-matrix fit of the existing $^{13}\text{C}(\alpha, n)^{16}\text{O}$ data, they got a result in agreement with [7]. Ambiguities on the reaction mechanism (direct transfer or compound nucleus), finite energy resolution, detection thresholds, background due to, for instance, ^{12}C impurities in enriched ^{13}C targets, ambiguity on optical potential parameters, node numbers and well geometry might be responsible for such inconsistencies between indirect measurements, making further measurements unavoidable.

The Trojan horse method (THM) allows one to study the $^{13}\text{C}(\alpha, n)^{16}\text{O}$ reaction free of Coulomb suppression and electron screening with no need of extrapolation (see [20] for a review on the method). In the THM, the low-energy cross section of a $A(x, c)C$ reaction is obtained by extracting the quasi-free (QF) contribution to a suitable $A(a, cC)s$ reaction. The use of a three-body reaction allows for a number of kinematic tests to separate the $A(a, cC)s$ channel from background reactions [20]. Similarly, the analysis of the reaction dynamics enables us to unambiguously single out the QF reaction mechanism [20]. In the case of resonance reactions, the modified R-matrix approach has been devised by A.M. Mukhamedzhanov [21] to extract the reduced widths γ from the THM reaction yield. In this framework, assuming that the $A(x, c)C$ reaction proceeds via isolated non-interfering resonances, the THM cross section is [22, 23]:

$$\frac{d^2\sigma}{dE_{xA}d\Omega_s} = \text{NF} \sum_i (2J_i + 1)$$

$$\times \left| \frac{\sqrt{k_f(E_{xA})}}{\mu_{cC}} \frac{\sqrt{2P_{l_i}(k_{cC}R_{cC})} M_i(p_{xA}R_{xA}) \gamma_{cC}^i \gamma_{xA}^i}{D_i(E_{xA})} \right|^2 \quad (1)$$

in the plane wave impulse approximation (PWIA), where NF is a normalization factor, J_i the spin of the i -th resonance, $k_f(E_{xA}) = \sqrt{2\mu_{cC}(E_{xA} + Q)}/\hbar$ (Q is the reaction Q -value, E_{xA} the $x-A$ -relative energy), P_{l_i} the penetration factor in l_i -wave, R_{xA} and R_{cC} the channel radii.

$$M_i(p_{xA}R_{xA}) = \left[(B_{xAi} - 1) j_{l_i}(\rho) - \rho \frac{\partial j_{l_i}(\rho)}{\partial \rho} \right]_{\rho=p_{xA}R_{xA}} \quad (2)$$

[24], where $j_{l_i}(\rho)$ is the spherical Bessel function, $p_{xA} = \sqrt{2\mu_{xA}(E_{xA} + B_{xs})}/\hbar$ (B_{xs} the binding energy of the $a = (xs)$ system), and B_{xAi} an arbitrary boundary condition chosen as in [21] to yield the observable resonance parameters. Finally, $D_i(E_{xA})$ is the standard R-matrix denominator in the case of two-level, one-channel R-matrix formulas [25]. In Eq.1, the same reduced widths appear as in the S(E)-factor, the only difference being the absence of any Coulomb or centrifugal penetration factor in the entrance channel. From the fitting of the experimental THM cross section they can be obtained and used to deduce the $^{13}\text{C}(\alpha, n)^{16}\text{O}$ astrophysical factor.

In this work, we will extend the THM to the analysis of sub-threshold resonances and extract the ANC $\tilde{C}_{\alpha^{13}\text{C}}^{17\text{O}(1/2^+)}$ of the -3 keV resonance from THM data, disclosing the deep connection between ANC and THM. Moreover, the neutron partial width Γ_n will be also inferred by means of Eq.1 and both parameters will be used to determine the influence of this resonance on the $^{13}\text{C}(\alpha, n)^{16}\text{O}$ reaction rate.

The experiment was performed at the John D. Fox Superconducting Linear Accelerator Facility at Florida State University, which delivered a 7.82 MeV, 1 mm spot ^6Li beam impinging onto a $53 \mu\text{g}/\text{cm}^2$, 99% ^{13}C enriched foil. Therefore, we used ^6Li , having a well known $\alpha + d$ structure, to transfer an α -particle to ^{13}C while d was emitted without interacting in QF kinematics. ^{16}O from the $^{13}\text{C}(\alpha, n)^{16}\text{O}$ sub-reaction and deuterons were detected, to maximize the detection efficiency and reduce systematic uncertainties. The detection setup consisted of five $5 \times 1 \text{ cm}^2$ position sensitive silicon detectors (PSD 1-5), having energy and position resolution 0.5% and 0.3 mm, respectively. Silicon ΔE detectors were placed in front of PSD 2-3 for particle identification.

The background-subtracted $\frac{d^2\sigma}{dE_{c.m.}d\Omega_d}$ cross section is displayed as full symbols in Fig.1. The error budget affecting experimental data comprises statistical, background subtraction and angular integration uncertainties. The horizontal error bars give the width of the $\alpha - ^{13}\text{C}$ relative-energy bins. Fig.1 clearly shows the presence of several resonances in the $^{13}\text{C}-\alpha$ relative energy spectrum, at $\sim -3 \text{ keV}$, $\sim 810 \text{ keV}$ and $\sim 1.02 \text{ MeV}$. These peaks correspond to ^{17}O states at 6.356 MeV ($J^\pi = 1/2^+$), 7.165 MeV ($J^\pi = 5/2^-$), 7.248 MeV

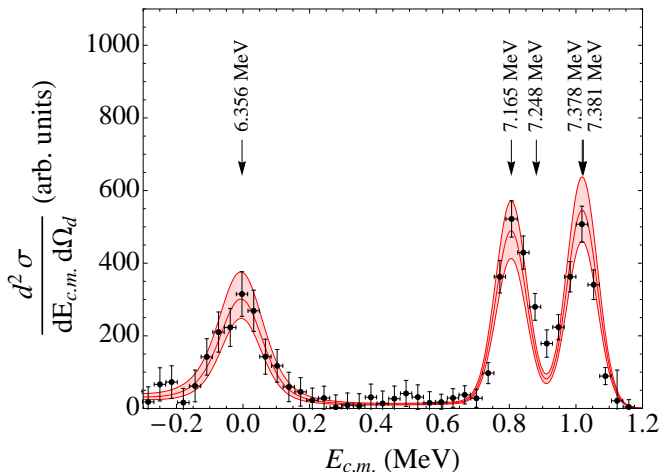


FIG. 1. Modified R-matrix fit of THM data (black symbols), integrated over $\theta_{c.m.}$. In the fit, the parameters of the resonances above 500 keV were kept fixed at the ones in [7]. The middle, top and bottom red lines are used for the best fit and the $\pm 1\sigma$ confidence interval, respectively, set by the experimental uncertainties (statistical, background subtraction and normalization).

($J^\pi = 3/2^+$), 7.378 MeV ($J^\pi = 5/2^+$) and 7.381 MeV ($J^\pi = 5/2^-$), as marked by arrows (resonance energies are taken from [7, 19]). As discussed in [22] and through a preliminary analysis based on Eq.1 and resonance parameters in [7], the 7.248 MeV and the 7.381 MeV states give minor contribution to the THM yield. A modified R-matrix analysis was then carried out.

Above 500 keV, where the influence of the -3 keV resonance is negligible, the reduced widths γ have been fixed to reproduce the partial widths Γ in [7]. This work has been chosen for reference as it combines a very large data set, reducing systematic errors possibly affecting some experimental cross sections. Such γ 's are used to calculate a modified R-matrix function to be superimposed on THM data, including all the ^{17}O levels contributing directly and through their interference between -0.3–1.2 MeV. The channel radii have been fixed to the ones in [7] ($R_{\alpha^{13}\text{C}} = 5.2$ fm and $R_{n^{16}\text{O}} = 4.0$ fm). The resulting cross section has been folded with a Gaussian having $\sigma = 46$ keV to account for energy resolution [26], as calculated from beam spot size and divergence, energy loss in the ΔE detectors, Al foil, target and dead layers, PSD intrinsic angular and energy resolution. Therefore, the normalization constant NF in Eq.1 is the only free parameter to match the modified R-matrix calculation with the indirect data. Fig.1 demonstrates the good agreement between the THM $\frac{d^2\sigma}{dE_{c.m.}d\Omega_d}$ cross section and the calculated one. To account for normalization error a band is specified in Fig.1, displaying the $\pm 1\sigma$ confidence interval of the scaling factor, obtained by adjusting NF to match the upper and lower tips of the data error bars.

Such an agreement is crucial as it serves as a validity

test of the method [27], besides providing for the normalization parameter NF. To cross check our approach, the FRESKO code [28] has been used to calculate the ratio of the peak values of the 810 keV and 1.02 MeV resonances in the DWBA. The same optical potential parameters as in [14] have been adopted. The DWBA calculations reproduce the experimental results within 9%, that is within the normalization error (17%), corroborating the present results by means of a more accurate approximation. Systematic errors due to the theoretical approach are less than 9%. An additional source of uncertainty is the accuracy of the R-matrix fit of [7], which is used for normalization. This is smaller than $\sim 5\%$, so it has been neglected in the following analysis as it is much smaller than the 17% normalization error.

Below $E_{c.m.} = 500$ keV, THM data clearly display the presence of a resonance located at -3 keV, corresponding to the 6.356 MeV ^{17}O level. For the first time this resonance has been observed in the $^{13}\text{C}(\alpha, n)^{16}\text{O}$ reaction, as it lays at negative $\alpha - ^{13}\text{C}$ relative energies. The modified R-matrix approach is employed to extract its resonance parameters by fitting the THM cross section. The same scaling factor as determined above has been used for $E_{c.m.} < 500$ keV, to ensure normalization to [7], and the same energy resolution, thus γ_n and γ_α are the only fitting parameters. The best fit curve is presented in Fig.1; an overall $\chi^2 = 1.28$ has been obtained. Uncertainties on the reduced widths and on modified R-matrix calculated cross section are made up of two components, a statistical error, connected to the scatter of data points below 500 keV, and normalization error, depending on the choice of NF due to the fitting of the data above 500 keV. The 1σ confidence region is shown in Fig.1 as a red band. From the reduced widths, the observable partial width $\Gamma_n^{1/2^+} = 83_{-12}^{+9}$ keV of the -3 keV resonance has been calculated, significantly smaller than the value usually adopted in the literature, 124 ± 12 keV [19], and reported in [7], 158 keV. The ANC $\tilde{C}_{\alpha^{13}\text{C}}^{17\text{O}(1/2^+)}$ of the -3 keV resonance was also established from the THM data. This is the first time that THM is used to derive the ANC of a sub-threshold resonance. Following the discussion in [29], we got $(\tilde{C}_{\alpha^{13}\text{C}}^{17\text{O}(1/2^+)})^2 = 6.7_{-0.6}^{+0.9} \text{ fm}^{-1}$ that is in agreement, within the uncertainties, with the ANC in [16, 17], but significantly larger than the ANC in [14, 15] (Tab.I). Here we infer both $\tilde{C}_{\alpha^{13}\text{C}}^{17\text{O}(1/2^+)}$ and $\Gamma_n^{1/2^+}$ from the same data set, so no resonance parameters from complementary works were necessary, as in previous investigations.

Introducing the THM reduced widths into a standard R-matrix code [25] the $^{13}\text{C}(\alpha, n)^{16}\text{O}$ S-factor is retrieved. The result is given in Fig.2, the red middle line being the best fit curve and the upper and lower red lines setting the recommended range allowed for by the statistical, normalization and data reduction uncertainties. For

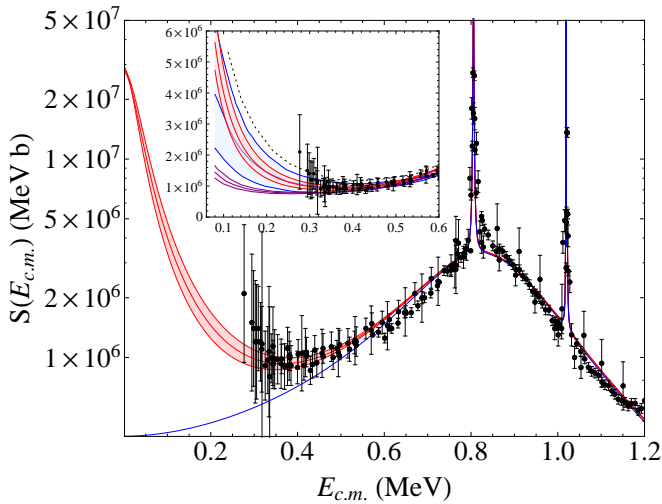


FIG. 2. R-matrix calculated S-factor (red middle line), obtained using the THM resonance parameters. The upper and lower red lines mark the range allowed for by the experimental errors, not including the uncertainty due to the accuracy of the R-matrix fit of [7]. The R-matrix S-factor, not including the resonance at -3 keV, is displayed by the blue line. Black points are the direct data normalized as in [7]. In the inset, the THM result is compared with some R-matrix extrapolations in the literature. The broad blue band underscores the extrapolation in [7]. Johnson et al. [14] calculation is given as a purple band (lowest band). Finally, a dotted line is used for Hale R-matrix S-factor [11].

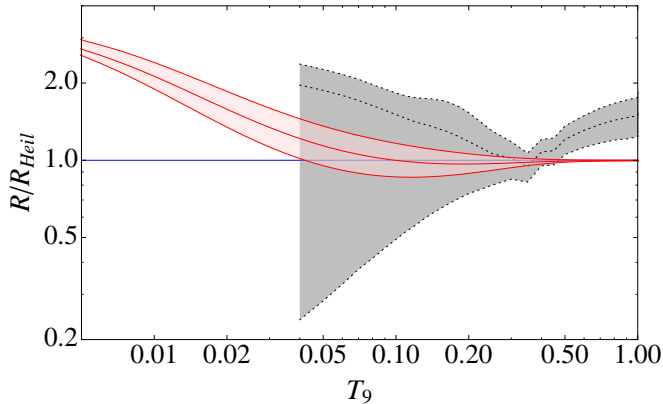


FIG. 3. Ratio of the THM (red band) and of the NACRE [12] (gray band) reaction rates to the Heil et al. one [7] (blue line). Temperature is given in units of 10^9 K.

comparison, the S-factor deprived of the contribution of the 6.356 MeV ^{17}O level is shown as a blue line. The black points represent the available direct $^{13}\text{C}(\alpha, n)^{16}\text{O}$ data scaled to match the high precision data of [7]. A very good agreement is found between the THM S(E)-factor and the direct data.

In Fig.2 the THM S(E)-factor (red band) is also compared with some of the available extrapolation of the

$^{13}\text{C}(\alpha, n)^{16}\text{O}$ astrophysical factor. In detail, the blue band indicates the extrapolations performed by [7], in very good agreement with the Breit-Wigner fit of [8] and the R-matrix S-factor of [17]. This band demonstrates the large uncertainties, about a factor of 2 at 100 keV, affecting extrapolations. The low purple band is used for [14], about a factor of 3 smaller than the extrapolation in [7], owing to the comparatively small ANC. By contrast, the R-matrix approach in [11] predicts a factor of 2 larger S-factor than [7]. A good agreement is found with the most recent extrapolations in [7, 17], within the large experimental uncertainties, though the THM recommended value at 100 keV is about 22% larger. Furthermore, the uncertainties affecting the S(E)-factor at astrophysical energies have been greatly reduced, $\sim 18\%$ at 100 keV, about 10 times smaller than in the literature. This enhanced accuracy is definitely attributable to the THM approach, as no extrapolation is used. The inclusion of $\sim 5\%$ uncertainty affecting the R-matrix fit of [7] marginally influences the present result, leading to a small increase of the total error to 19% at 100 keV.

Below ~ 150 keV, a larger S(E)-factor is obtained than in [7], up to a factor of 3.7 at zero energy, due to the THM $\tilde{C}_{\alpha^{13}\text{C}}^{17\text{O}(1/2^+)}$ of the -3 keV resonance. This result might have important consequences on background estimate in neutrino detectors [30] and on the s-process, as it might cause a different neutron density and a lower ignition temperature of the $^{13}\text{C}(\alpha, n)^{16}\text{O}$ reaction because of the increased ^{13}C destruction rate at low energies. The reaction rate has been calculated by means of standard equations [5] and compared with the most recent one [7], in agreement with the rate in [31] widely used in stellar evolutionary and nucleosynthesis codes. While at $0.9 \cdot 10^8$ K a difference of only 1% is found, at 10^7 K the THM reaction rate is two times larger than in [7], up to a factor of 3 for lower temperatures (Fig.3). Moreover, the present reaction rate is affected by a much smaller error (18%) than the NACRE one, namely +17% and -69% [12] (Fig.3), and slightly smaller than the Heil et al. one, about 22% [7]. This result strongly calls for an exhaustive analysis of the astrophysical consequences. To set an upper limit to the changes due to the THM reaction rate, the rate in [8] has been multiplied by a factor of 3. Adopting the s-process nucleosynthesis framework in [32], ^{86}Kr , ^{87}Rb , ^{96}Zr and ^{142}Ce show an increase by at least 30%, as they are located after an unstable isotope in the nuclear chart and the increase of the neutron density favors their production. These changes might be very important in the understanding of the solar distribution of neutron capture nuclei.

In summary, in this letter we report on an innovative experimental and theoretical approach allowing to achieve a presently unparalleled accuracy in the investigation of sub-threshold resonances. This approach combines the THM and ANC indirect methods to get all the

resonance parameters and the $S(E)$ -factor down to zero energy, with no need of extrapolation. It is a very promising approach as it can be implemented for reactions induced by stable and radioactive beams, to study charged particle and radiative capture reactions. This technique has been applied to the investigation of $^{13}\text{C}(\alpha, n)^{16}\text{O}$ reaction that represents a pivotal reaction in the nucleosynthesis of heavy nuclei. A larger $S(E)$ factor is obtained below ~ 100 keV than in the literature, owing to the larger ANC of the -3 keV resonance. Interesting consequences for the s-process have been envisaged, calling for a deeper investigation of AGB nucleosynthesis.

The work was supported by the Italian MIUR under grant No. RBFR082838. G.G.K. acknowledges the support by OTKA (PD104664) and the János Bolyai Research Scholarship of the Hungarian Academy of Sciences. A.M.M. acknowledges the support by US Department of Energy under Grant Nos. DE-FG02-93ER40773, and DE-SC0004958 (topical collaboration TORUS) and NSF under Grant No. PHY-0852653. O.T. is grateful to Fondazione Cassa di Risparmio di Perugia for financial support.

* lacognata@lns.infn.it

- [1] B. Meyer, *Annu. Rev. Astron. Astrophys.*, **32**, 153 (1994).
- [2] F. Käppeler, R. Gallino, S. Bisterzo, and W. Aoki, *Reviews of Modern Physics*, **83**, 157 (2011).
- [3] R. Gallino *et al.*, *Astrophys. J.*, **497**, 388 (1998).
- [4] M. Busso, R. Gallino, and G. J. Wasserburg, *Annual Review of Astronomy and Astrophysics*, **37**, 239 (1999).
- [5] C. Iliadis, *Nuclear Physics of Stars* (Wiley-VCH Verlag, 2007).
- [6] C. E. Rolfs and W. S. Rodney, *Cauldrons in the cosmos* (University of Chicago Press, Chicago, IL, 1988).
- [7] M. Heil *et al.*, *Phys. Rev. C*, **78**, 025803 (2008).
- [8] H. W. Drotleff *et al.*, *Astrophys. J.*, **414**, 735 (1993).
- [9] M. La Cognata *et al.*, *Phys. Rev. C*, **72**, 065802 (2005).
- [10] A. M. Mukhamedzhanov, M. La Cognata, and V. Kroha, *Phys. Rev. C*, **83**, 044604 (2011).
- [11] G. M. Hale, *Nucl. Phys. A*, **621**, 177 (1997).
- [12] C. Angulo *et al.*, *Nuclear Physics A*, **656**, 3 (1999).
- [13] M. Dufour and P. Descouvemont, *Phys. Rev. C*, **72**, 015801 (2005).
- [14] E. D. Johnson *et al.*, *Physical Review Letters*, **97**, 192701 (2006).
- [15] S. Kubono *et al.*, *Phys. Rev. Lett.*, **90**, 062501 (2003).
- [16] N. Keeley, K. W. Kemper, and D. T. Khoa, *Nucl. Phys. A*, **726**, 159 (2003).
- [17] M. G. Pellegriti *et al.*, *Phys. Rev. C*, **77**, 042801 (2008).
- [18] A. M. Mukhamedzhanov *et al.*, *Phys. Rev. C*, **56**, 1302 (1997).
- [19] D. R. Tilley, H. R. Weller, and C. M. Cheves, *Nucl. Phys. A*, **564**, 1 (1993).
- [20] C. Spitaleri, A. M. Mukhamedzhanov, L. D. Blokhintsev, M. L. Cognata, R. G. Pizzone, and A. Tumino, *Physics of Atomic Nuclei*, **74**, 1725 (2011).
- [21] M. La Cognata, C. Spitaleri, and A. M. Mukhamedzhanov, *Astrophys. J.*, **723**, 1512 (2010).
- [22] M. La Cognata *et al.*, *Astrophys. J.*, **739**, L54 (2011).
- [23] A. M. Mukhamedzhanov, L. D. Blokhintsev, B. F. Irgaziev, A. S. Kadyrov, M. La Cognata, C. Spitaleri, and R. E. Tribble, *Journal of Physics G Nuclear Physics*, **35**, 014016 (2008).
- [24] A. M. Mukhamedzhanov, *Phys. Rev. C*, **84**, 044616 (2011).
- [25] A. M. Lane and R. G. Thomas, *Reviews of Modern Physics*, **30**, 257 (1958).
- [26] M. La Cognata, V. Z. Goldberg, A. M. Mukhamedzhanov, C. Spitaleri, and R. E. Tribble, *Phys. Rev. C*, **80**, 012801 (2009).
- [27] M. La Cognata *et al.*, *Nucl. Phys. A*, **834** (2010).
- [28] I. J. Thompson, *Comput. Phys. Rep.*, **7** (1988).
- [29] A. M. Mukhamedzhanov and R. E. Tribble, *Phys. Rev. C*, **59**, 3418 (1999).
- [30] S. Harissopulos, H. W. Becker, J. W. Hammer, A. Lagoyannis, C. Rolfs, and F. Strieder, *Phys. Rev. C*, **72**, 062801 (2005).
- [31] A. Denker and J. Hammer, in *Nuclei in the Cosmos 1994*, edited by M. Busso, R. Gallino, and C. Raiteri (AIP, New York, 1995) p. 255.
- [32] E. Maiorca *et al.*, *Astrophys. J.*, **747**, 53 (2012).